Charge-Exchange Plasma Contamination on SMART-1: First Measurements and Model Verification

M. Tajmar*, W. Meissl
Space Propulsion, ARC Seibersdorf research, A-2444 Seibersdorf Austria

J. González del Amo, B. Foing, H. Laakso
ESA-ESTEC, Keplerlaan 1, 2200 AG Noordwijk, The Netherlands

G. Noci, M. Capacci
LABEN Proel, Firenze, Italy

A. Mälkki, W. Schmidt
Finnish Meteorological Institute, Helsinki, Finland

F. Darnon
CNES, Toulouse, France

SMART-1, launched in fall 2003, is Europe's first moon satellite. It shall demonstrate Solar-Electric Propulsion using a PPS-1350 hall thruster. One of the main mission investigations is the characterization of the thruster's charge-exchange ion environment. Two instruments support this analysis: EPDP, consisting of a Langmuir probe, RPA analyser and a solar cell sample, and SPEDE, consisting of two current collection spheres supported by two short booms. ARC Seibersdorf research developed a Particle-In-Cell plasma simulation to support and predict the thruster's induced plasma environment around SMART-1. This paper will give an overview of the modeling approach and a comparison of the model will test results gained during the STENTOR ground test campaign using a similar thruster. We will also report a first interpretation of the measurements from EPDP and SPEDE on SMART-1 and will compare them with the actual model predictions. This analysis shall be used to actually validate the simulation tool to reliably predict charge-exchange plasma environments on future missions using electric propulsion.

I. Introduction

THE first of the Small Missions for Advanced Research in Technology (SMART-1) of the ESA Horizons 2000 scientific programme is dedicated to the testing of new technologies for preparing future cornerstone missions, using Solar-Electric Propulsion in Deep Space[1]. SMART-1 was launched on the 27th of September 2003 as an Ariane 5 cyclade-like auxilary payload and uses a Hall thruster (PPS-1350) built by SEP[2,3] to fly to the moon. The first moon orbit is expected to be reached by late November 2004.

* Principal Scientist, Space Propulsion, also Lecturer, Department for Aerospace Engineering, Vienna University of Technology, Austria, Tel: +43-50550-3142, Fax: +43-50550-3366, Email: martin.tajmar@arcs.ac.at, Member AIAA.

This is the first time of primary electric propulsion on a European spacecraft. Hence, the evaluation of the Hall thruster impact on the spacecraft and its instruments is one of the primary scientific objectives. In addition to primary beam ions, electric propulsion thrusters create a low-energy charge-exchange ion environment. The distribution of these ions is strongly affected by the potential distribution near the spacecraft being a possible contamination source for instruments and solar arrays. Although charge-exchange plasma interactions have been a subject of extensive experimental and theoretical studies[4-6], there have been few comprehensive in-flight investigations due to the lack of flight opportunities. The first interplanetary spacecraft using solar electric propulsion is Deep Space One[6] using the NASA Solar Electric Propulsion Technology Application Readiness (NSTAR) ion engine. SMART-1 is the first interplanetary mission using a Hall thruster.

ARC Seibersdorf research previously developed a 3D Particle-In-Cell (PIC) code to study the charge-exchange environment around the SMART-1 satellite[7-10]. The code was successfully verified with ground test data both in the near and far field[11]. In this paper, we extend our verification analysis to the STENTOR ground test campaign, which used a thruster and operating conditions similar to those on SMART-1. Furthermore, the code was extended to include a variable electron temperature model, more collision models and an enhanced model of the virtual RPA analyser (including angle or orientation). The updated code was then applied to the SMART-1 case and compared with the first in-flight measurement results. The agreement from the previously published and updated results with flight data is very good.

II. Spacecraft Overview

SMART-1 is a cube spacecraft with the dimensions 1.15x1.15x1 m and two solar arrays stretching out from two opposite sides giving a total length of 8 m. A schematic location of the thruster and the electric propulsion related instruments is shown in **Fig. 1**. The PPS-1350 Hall effect thruster operates at a specific impulse of 1640 seconds delivering a maximum thrust of 70 mN using Xenon gas as propellant (see **Table 1**). Several plasma sensors onboard SMART-1 characterise the ambient plasma and the effects on the low-energy charge-exchange plasma emitted by the Hall thruster. In this section, we will give an overview of the instruments involved in the evaluation of the spacecraft/environment interactions related to electric propulsion:

Parameters	PPS-1350 Thruster
Thrust	70 mN
Voltage	350 V
Current	3.8 A
Mass Flow Rate	4.2 mg/s
Specific Impulse	1640 s
Power	1350 W
Total Efficiency	51 %

Table 1. PPS-1350-G Performance Parameters on SMART-1.

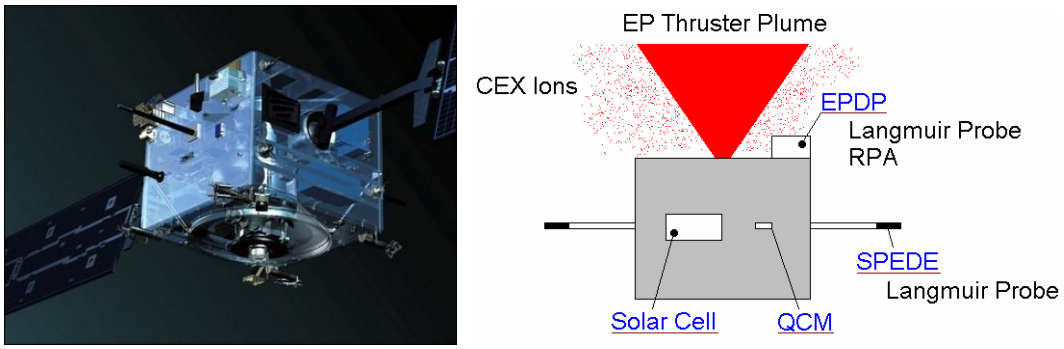

Figure 1. SMART-1 Illustration (left) and Schematic Instrument Location on SMART-1 (right).

1. Electric Propulsion Diagnostic Package (EPDP)

This package consists of four instruments outside the primary ion beam (Langmuir probe, Retarding Potential Analyser, Solar Cell Sample, and Quartz Crystal Microbalance) aiming at characterising the charge-exchange ion environment around the spacecraft. The instrument requirements are summarised in **Table 2**.

Physical Parameters	Instrument Requirements
Plasma Density	$10^{13} – 3.10^{14}$ m^{-3}
Ion Energy	0 – 400 eV
Electron Temperature	1.7 – 3.5 eV
Plasma Potential	-150 – 100 V
Ion Current Density	0.002 – 0.05 mA/cm^2
Deposition	0 – 0.29 mg/cm^2

Table 2. EPDP Instrument Specifications.

- Langmuir Probe: The spherical Langmuir probe is located 55 cm next to the Hall thruster (**Fig. 2**). This sensor provides information about the plasma potential, the electron density and the temperature respectively. The charge-exchange ion trajectories are determined by the potential distribution created by space charge effects around the spacecraft. Outside the primary beam ions, the potential is composed of the space charges from the charge-exchange ions and the neutraliser electrons. Hence, the Langmuir probe data provides useful information on the electron behaviour and therefore on the potential and charge-exchange distribution near the thruster.

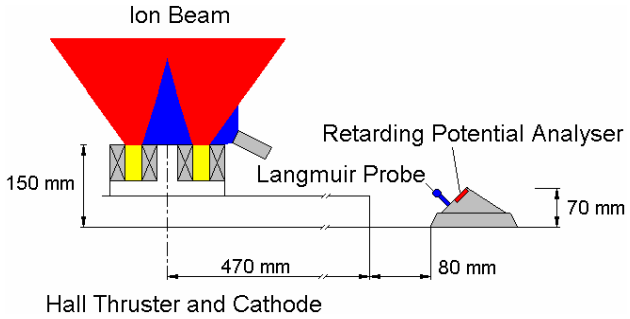

I.

Figure 2. EPDP Location.

- Retarding Potential Analyser (RPA): This sensor is located next to the Langmuir probe on the same probe assembly (**Fig. 2**). The retarding potential analyser measures the ion energy and current density distribution passing through a grid structure. The charge-exchange ion energy is of crucial importance to predict sputtering phenomena on the spacecraft surface.

- Solar Cell Sample: A solar cell sample will be mounted on the –X panel of SMART-1 to study possible degradation due to the operation of the electric propulsion system (see **Fig. 1**). If power losses are observed, they also provide information of the charge-exchange ion density and energy related to sputtering of the solar cell's cover glass causing the degradation. The presence of charge-exchange ions in this location is, however, unlikely. As the simulation results show, the charge-exchange ions are expected to expand radially from the primary ion beam. The only possible mechanism to attract ions to the solar panel location is a change in the ambient potential structure or large different floating potential conditions depending on the orbit and eclipses. Hence, the analysis of these data is crucially linked to the Langmuir probe and the SPEDE sensors which provide information about the ambient plasma environment and the spacecraft potential, as shown later.

- Quarz Crystal Microbalance (QCM): This sensor is located next to the solar cell sample to monitor possible deposition of propellant ions during thruster operation (see **Fig. 1**). Deposition is especially important for optical instruments like cameras. As already mentioned above, the presence of charge-exchange ions at this location is unlikely. Similar measurements in Deep Space One indicated the presence of a charge-exchange ion flux to a Langmuir probe on the opposite side of the thruster[6]. However, changes in the floating potential were not monitored. The flux was orders of magnitude below the solar wind flux and occurred only at certain high thrust level conditions. If sensor data appears during thruster operation, QCM data will also contribute to a better understanding of the interaction between the charge-exchange ions and the ambient plasma environment.

2. Spacecraft Potential, Electron and Dust Experiment (SPEDE)

The SPEDE experiment consists of two electric sensors of cylindrical shape mounted on the ends of two 60-cm booms. Each sensor can work either in a Langmuir (LP) mode or in an electric field (EF) mode.

When operated in an EF mode, the sensor is current-biased, and both the spacecraft potential and wave electric fields can be monitored. As already pointed out, large variations in the spacecraft potential affect the charge-exchange ions distribution. These measurements will aid the analysis of possible contamination detected by the solar cell sample and the QCM. Also, gas molecules absorped on the spacecraft will later be slowly desorped, resulting in enhanced plasma wave activity[12].

Using the potential measurement of an EF sensor and the electron temperature from the EPDP Langmuir probe, we can even estimate the charge-exchange ion density, assuming a Boltzmann energy distribution of the neutralising electrons.

In an LP mode, the sensor is voltage-biased in order to monitor the variation of the electron flux. An increase of the electron flux would also indicate the presence of charge-exchange ions in a quasi-neutral plasma.

III. Computational Model

The code is based on a three-dimensional hybrid Particle-In-Cell Code[13,14] (PIC-MCC) with Monte-Carlo collision models, treating the ions and neutrals as test particles. The detailed physical and numerical models used are described in detail in Refs. 7-11.

For the plasma densities and temperatures produced by a Hall thruster, the electrons can be treated as collisionless. Therefore, one can calculate the potential in the beam using the Boltzmann relationship assuming a quasi-neutral plasma using

$$n_i \approx n_e = n_{ref} \cdot \exp\left(\frac{e\phi}{kT_e}\right) \quad , \tag{1}$$

where n_i is the ion density, T_e the electron temperature, ϕ the potential, and n_{ref} the reference electron density where the potential is set to zero. The previous code assumed a constant electron temperature throughout the beam. Although this is a good approximation for obtaining reasonable results, a more refined model is necessary to interpret the EPDP data in detail. Therefore, a variable electron temperature model was implemented following the approach from VanGilder[15]. Following the law for adiabatic fluids, the electron temperature can be expressed as a function of the ion (electron) density:

$$T_e = c \cdot n^{\gamma-1} \quad . \tag{2}$$

The constants c and γ are chosen to fit experimental data on electron densities and temperatures. In addition to the refinement in the electron temperature model, also the collision models were updated. **Table 3** lists all implemented collisions, the respective equations to calculate the cross sections as well as the references. Almost all models use the data from Rapp and Francis[17] to calculate the cross section for Xenon ions and neutrals. However, Miller et al[18] recently reported new measurements which were implemented in the model. The $Xe^{++} + Xe$ asymmetric charge exchange cross section is taken from experimental values obtained by Miller[18] et al. and the single electron recombination cross section is a rough estimate suggested by Dressler[19]. The last two cross sections have a large uncertainty, but they are also extremely small and their implementation was performed mainly to see if there was any visible effect coming from them. King et al[20,21] pointed out the importance of symmetric charge-exchange collisions between $Xe^{++} + Xe^{+}$ ions to explain the high energy tail observed on RPAs in the backflow region from Hall thrusters. For the first time, we implemented such a collision in a numerical model to further investigate this effect. As there are no experimental measurements available, the cross section was extrapolated from data on hydrogen using a model described in Ref. 22. According to this analysis, the $Xe^{++} + Xe^{+}$ collision cross section is about a factor of 3 below the $Xe^{+} + Xe$ CEX collision cross section.

Name	Formula	Cross Section	Reference
(Xe^+, Xe) CEX	$Xe^+_{fast} + Xe_{slow} \Rightarrow Xe^+_{slow} + Xe_{fast}$	$\sigma = a_1 - b_1 \cdot \ln(v_{rel})$	Miller[18]
(Xe^{++}, Xe) CEX	$Xe^{++}_{fast} + Xe_{slow} \Rightarrow Xe^{++}_{slow} + Xe_{fast}$	$\sigma = a_2 - b_2 \cdot \ln(v_{rel})$	Miller[18]
(Xe^+, Xe) scattering	direction change	$\sigma = \frac{c}{v_{rel}}$	Dalgarno[16]
(Xe^{++}, Xe) scattering	direction change	$\sigma = 2 \cdot \frac{c}{v_{rel}}$	Dalgarno[16]
(Xe^{++}, Xe^+) CEX	$Xe^{++}_{fast} + Xe^+_{slow} \Rightarrow Xe^{++}_{slow} + Xe^+_{fast}$	$\sigma = a_3 - b_3 \cdot \ln(v_{rel})$	Tharamel[22]
Asymmetric CEX	$Xe^{++}_{fast} + Xe_{slow} \Rightarrow Xe^+_{slow} + Xe^+_{fast}$	$1\,\mathring{A}^2 \le \sigma \le 3\,\mathring{A}^2$	Miller[18]
Xe^{++} + e^- recomb.	$Xe^{++} + e^- \Rightarrow Xe^+$	$d \cdot \sqrt{T_e}$	Dressler[19]

where a_1=1.71 x10^{-18}, b_1 =1.18 x10^{-19}, a_2=1.03 x10^{-18}, b_2=7.7 x10^{-20}, a_3=4.32 x10^{-19}, b_3 =2.8 x10^{-20}, c= 6.42 x10^{-16} and d=2 x10^{-18}.

Table 3. Implemented Collisions.

Experimental Langmuir probe data like electron temperature, electron and ion densities or plasma potential can easily be compared with the values obtained at the relevant grid node. For comparison of retarding potential analyzer (RPA) or Faraday cup data, virtual instruments were created that simulate the response of the real plasma diagnostic package, EPDP. The degree of freedom for the virtual RPAs was enhanced and it is now possible to rotate them around their own axis. Furthermore, the collision query for particles hitting the RPA was adapted so that for instruments well outside the main beam, the effect of the grounded instrument attracting slow ions is now taken into account. For main beam ions which will not be affected by a potential drop of about 20 V, the angle of incidence of the ion hitting the RPA surface will correctly influence the generated peak.

IV. Ground Test Verification (STENTOR Campaign)

The French Satellite STENTOR, unfortunately lost in an Ariane 5 launch failure in 2000, had two Hall thrusters on board; an SPT-100 and, like SMART-1, a PPS-1350 engine. The same plasma diagnostic package (EPDP) was also to be used. In preparation for the mission, an SPT-100 used in a PPS-1350 like configuration (see **Table 4**) and the EPDP were tested extensively. Data gained in this campaign was compared to our simulations for model verification purposes. Additionally, the code was systematically tested for self-consistency by manipulating relevant input parameters and observing their effect on the simulation.

Parameter	PPS 1350 N condition
Thruster used	SPT 100-ML
Vacuum chamber pressure [mbar]	2.5x10^{-5}
Discharge voltage [V]	350
U_{Anode} [V]	335
$U_{Cathode}$ [V]	-15
Discharge current [A]	4.28
Anode mass flow rate [mg/s]	5.03
Cathode mass flow rate [mg/s]	0.44

Table 4. Experimental Setup Parameters for STENTOR Ground Test Campaign.

The tests were performed in a vacuum chamber at CNRS in France [23] which is able to maintain a pressure of 2.5x10^{-5} mbar when the thruster is firing. This neutral background is large compared to the neutral particles coming from the thruster itself, and therefore has a considerable effect on the CEX plasma densities and behavior.

The STENTOR ground campaign consisted of several RPA measurements at various positions both inside and outside the main beam, yet all within 1.2 meters of distance to the thruster. This matches the typical dimensions of our simulation domain. We are able to demonstrate the accuracy of our plasma simulation software with respect to the energy distribution in the beam. As seen in **Fig. 3**, for RPA's within the main beam, the agreement between predicted energy peaks and the experiment is satisfactory. Unfortunately, there is no data available on the energy distribution of the ions created in the PPS-1350 like thruster. The full RPA curve for a position of 60° off the main beam axis is shown in **Fig. 4**. The CEX ions peak was predicted correctly.

As a conclusion, the code successfully predicted the conditions of the hall thruster run in a PPS-1350 like configuration.

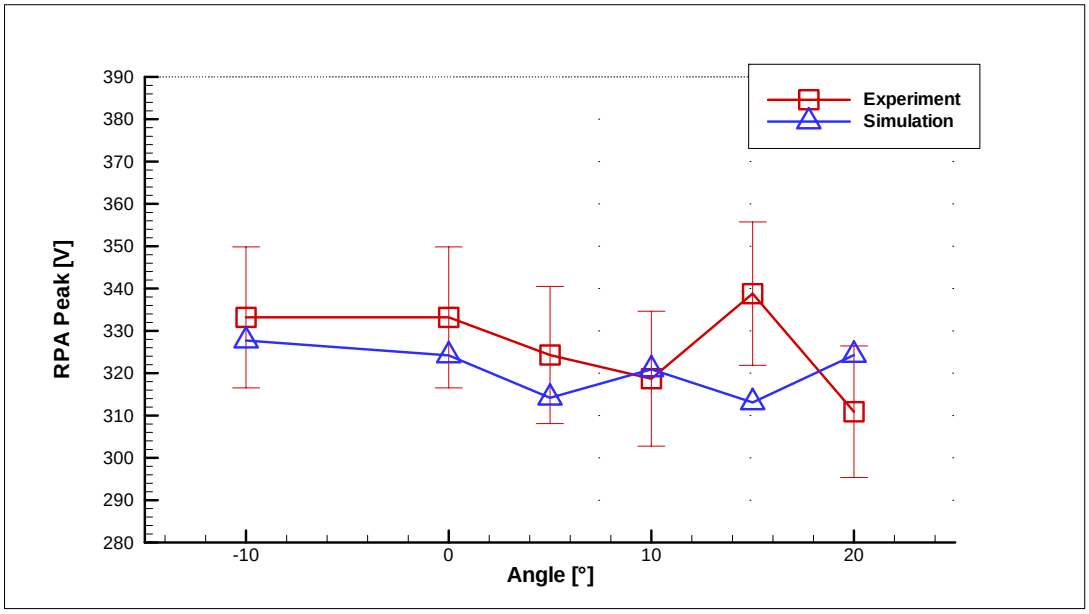

Figure 3. RPA Peak Energy Comparison between Simulation and STENTOR Measurements for PPS-1350 Thruster Conditions.

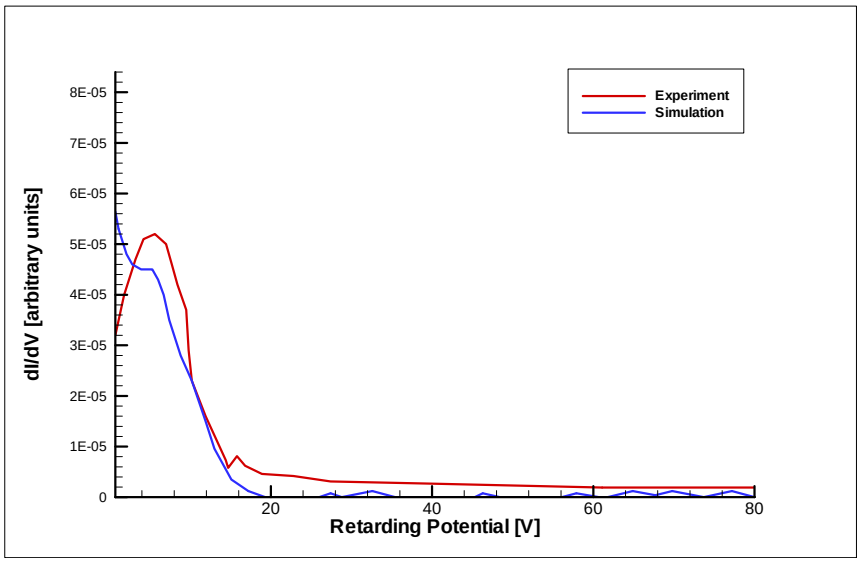

Figure 4. RPA Comparison at α=60°.

V. Simulation of SMART-1 Case and Comparison with Flight Data

Both constant (CT) and variable electron temperature (VT) models were used to simulate the SMART-1 case (see **Table 1**). The total ion and neutral densities for both cases are shown in **Figs. 5** and **6** respectively. It can be clearly seen that the VT model creates a stronger asymmetry triggered by the neutrals emitted by the cathode (see **Fig. 7 Left**). The enhancement of the asymmetry is due to the higher electron temperatures, which also cause a larger potential that pushes the charge-exchange ions out of the beam. The electron temperature profile for the VT model is shown in **Fig. 7 Right**. It is ranging from 4 eV at the exit of the Hall thruster (which is also the choice for the VT model) to about 10 eV at the ion density peak in front of the thruster. At the position of the EPDP, the electron temperature is going to below 1 eV, which is much more realistic compared to the CT model.

A comparison between the measurements of the EPDP and the simulation results is given in **Table 5**. This comparison also includes the model results previously published as preparation for the SMART-1 data analysis[9]. The fit between the observed and modelled ion and electron densities is better than one order of magnitude. Of course the VT model gives a much better fit (within 10%) of the electron temperature measured on SMART-1 and the one obtained from the model. The new model densities are generally larger than the previous one due to the implementation of the new CEX cross sections, which are also larger that the ones previously used. The plasma potential obtained from the simulations depends on the choice of the reference density, defining where the potential is set to zero. Only in the case of the VT model, the obtained potential was positive (about 2 V). A much better guess of the plasma potential is the peak obtained from the RPA, which defines the upper limit of the plasma potential. In this case, the fit between model and measurement is very good.

The floating potential of the EPDP Langmuir probe (LP) and the cathode reference potential (CRP) from the thruster is plotted together with the obtained spacecraft potential in **Fig. 9**. It can be seen that both LP and CRP vary together over the orbit. The reason for this is still under investigation. Possible explanations include interaction with the solar arrays or photoemission of the probes.

Also the RPA peaks measured by the EPDP follow this cycle at a constant offset of +18 V. Therefore, when comparing the RPA measurements with the simulation, the 18 V offset has to be subtracted as ions would gain this additional energy during collection which is not simulated by the model. The reason for this offset is that the first grid of the RPA is grounded to the satellite. Therefore, the ions gain an additional energy due to the difference of the local plasma potential and the spacecraft potential. A comparison between the RPA (shifted by -18 V, measured on 30.12.2003) and the model results is shown in **Fig. 10**. The agreement with the CT model and the previously published results up to 30 V is nearly perfect. The high energy up to 60 V is not predicted by the model. The VT model predicts a slightly higher peak (about 5 V) compared to the CT model and the measurements.

Comparing the CT model with the previously published results, the difference is very small. This suggests that the collision processes studies so far have little influence on the charge-exchange plasma. Modelling work is continuing to better fit the VT model to the RPA peak and to refine the $Xe^{++} + Xe^{+}$ collision processes which are believed to explain the high energy tail as outlined previously.

As the signal processing and data analysis from the SPEDE instrument is still ongoing, we will include a discussion about SPEDE in a later publication.

	SMART-1 Data	**Old Values**	**constant T_e**	**variable T_e**
Ion Density [m^{-3}]	$6 – 8\ 10^{13}$	$5 – 7\ 10^{13}$	$1 – 2\ 10^{14}$	$0.5 – 1.5\ 10^{14}$
Electron Density [m^{-3}]	$2.5 – 3.7\ 10^{13}$	$5 – 7\ 10^{13}$	$1 – 2\ 10^{14}$	$0.5 – 1.5\ 10^{14}$
Floating Potential [V]	-2 – 5	N/A	N/A	N/A
Plasma Potential*	20 – 27	-7 – -15	-7	2
RPA Peak [V]	19 (+18 V)	20	18.5	26
T_e [eV]	0.6 – 0.7	constant (4)	constant (4)	0.76

* Simulated plasma potentials depend on choice of reference potential in electron temperature model. Real plasma potentials will be positive up to the RPA peak ($V_{p,simulated} \cong 0 – 20$ V) .

Table 5. Data comparison at EPDP location.

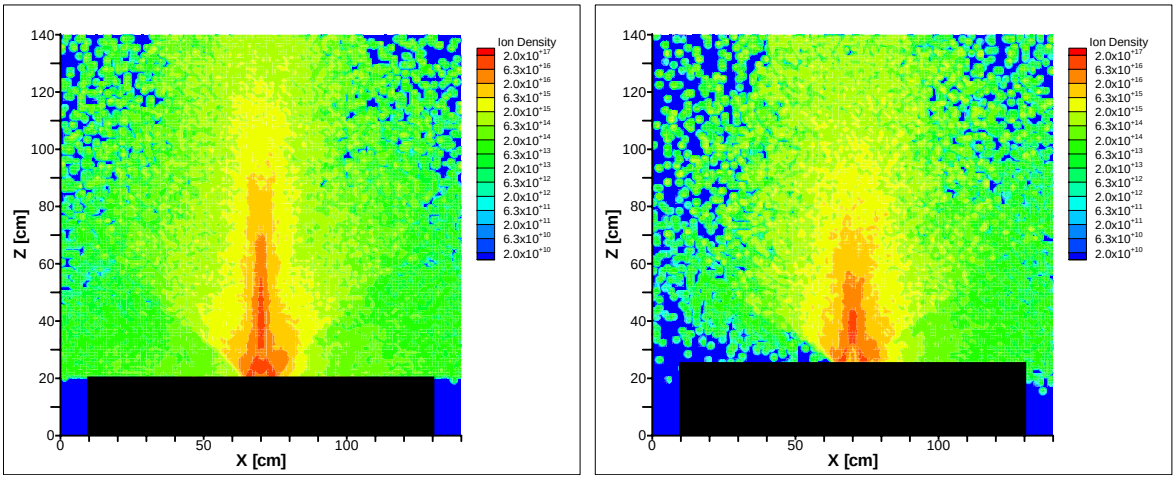

Figure 5. Total Ion Density using Constant (Left) and Variable Electron Temperature Model (Right).

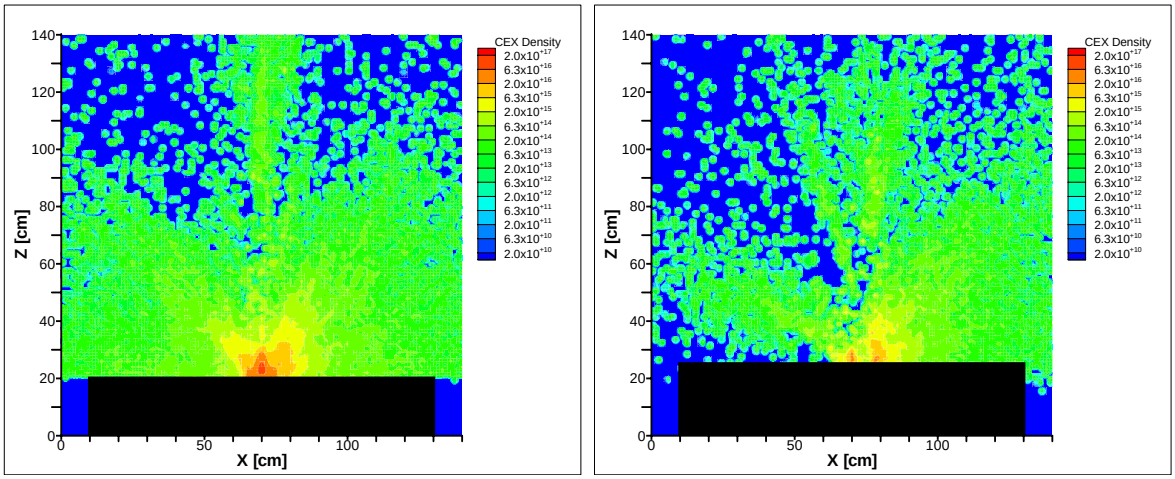

Figure 6. CEX Ion Density using Constant (Left) and Variable Electron Temperature Model (Right).

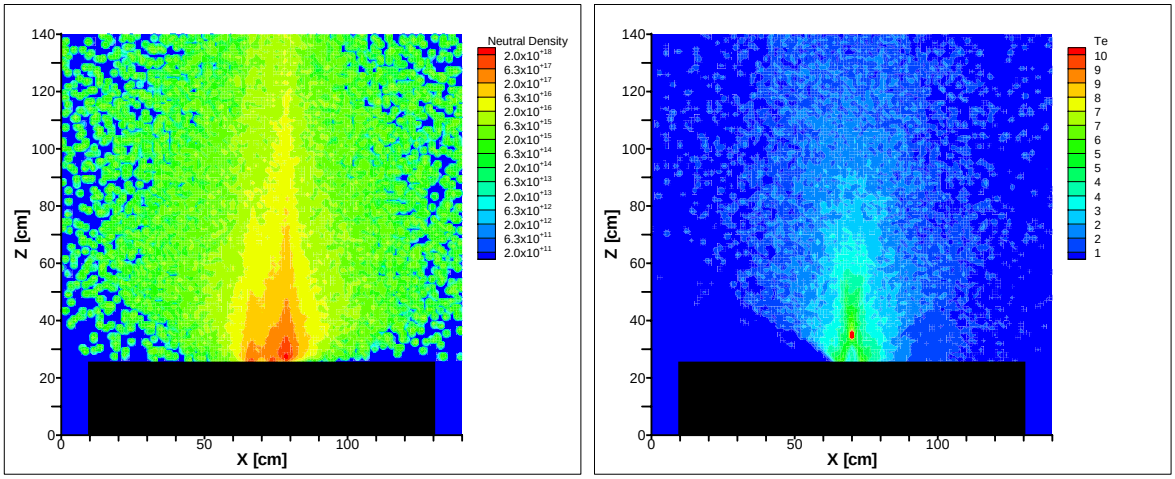

Figure 7. Neutral Density (Left) and Electron Temperature in Variable Electron Temperature Model (Right).

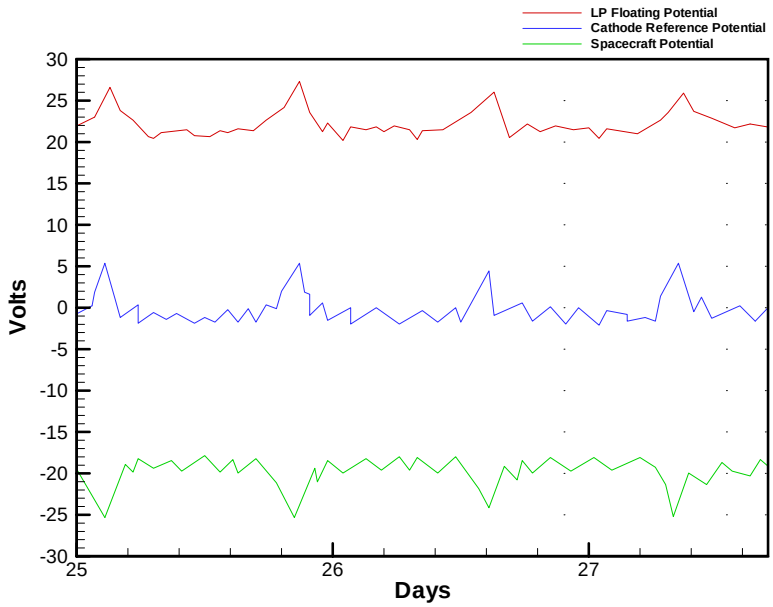

Figure 9. Comparison of Measured Potentials on SMART-1 (LP Floating Potential, Cathode Reference Potential and Spacecraft Potential).

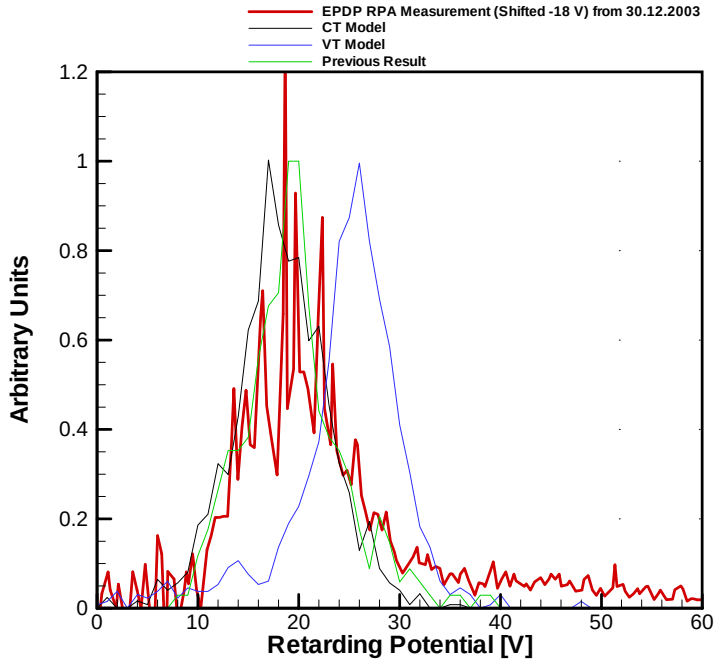

Figure10. Comparison of all Models with RPA Measurement from SMART-1.

VI. Conclusion

The 3D PIC code developed for SMART-1 accurately predicts the charge-exchange plasma environment around the spacecraft. The model predictions are very close to the actual flight measurements. Future work will include refinements on the variable electron temperature model, refinements for the collision models to better explain the high energy tail in the RPA measurements above 30 V and a study on the potential oscillations. In general, according to our modelling results, no significant CEX plasma interaction with the spacecraft is seen from both measurements and model, which is an important result for future electric propulsion satellites.

Acknowledgments

This work was funded by the Austrian Space Agency.

References

[1]Racca, G.D., et al, "SMART-1 Mission Description and Development Status", Planetary and Space Science, Vol. 50, 2002, pp. 1323-1337

[2]Valentian, D., and Maslennikov, N., "The PPS 1350 Program," *International Electric Propulsion Conference*, IEPC-97-134, Aug. 1997

[3]Lyszyk, M., Klinger, E., Secheresse, O., Bugeat, J.P., Valentian, D., Cadiou, A., Beltan, T., and Gelas, C., "Qualification Status of the PPS1350 Plasma Thruster," AIAA Paper 99-2278, June 1999

[4]Carruth, M., Ed., "Experimental and Analytical Evaluation of Ion Thruster/Spacecraft Interactions", *JPL Publication* 80-92, 1981

[5]Tajmar, M., Rüdenauer, F., and Fehringer, M., "Backflow Contamination of Indium Liquid-Metal Ion Emitters (LMIE): Numerical Simulations", *International Electric Propulsion Conference*, IEPC-99-070, Oct. 1999

[6]Wang, J., Brinza, D.E., Young, D.T., Nordhold, J.E., Polk, J.E., Henry, M.D., Goldstein, R., Hanley, J.J., Lawrence, D.J., and Shappiro, M., "Deep Space One Investigations of Ion Propulsion Plasma Environment", Journal of Propulsion and Power, Vol. 37, No. 5, 2000, pp. 545-555

[7]Tajmar, M., Gonzalez, J., and Hilgers, A., "Modelling of Spacecraft-Environment Interactions on SMART-1", *AIAA Joint Propulsion Conference*, AIAA 2000-3526, 2000

[8]Tajmar, M., Gonzalez, J., Foing, B., Marini, A., Noci, G., and Laakso, H., "Modelling of the Electric Propulsion Induced Plasma Environment on SMART-1", Proceedings of the 7th Spacecraft Charging Technology Conference, ESTEC, 2001

[9]Tajmar, M., Gonzalez, J., and Hilgers, A., "Modelling of Spacecraft-Environment Interactions on SMART-1", *AIAA Journal of Spacecraft and Rockets*, Vol. 38, No. 3, 2001, pp. 393-399

[10]Tajmar, M., Gonzalez, J., Saccoccia, G., Noci, G., and Laasko, H., "Plasma Diagnostics and Simulation for the SMART-1 Mission", *Planetary and Space Science*, Vol. 50, No. 14-15, pp. 1355-1360, 2002

[11]Tajmar, M., Gonzalez, J., Estublier, D., and Saccoccia, G., "Modelling and Experimental Verification of Hall and Ion Thrusters at ESTEC", Proceedings of the 3rd Spacecraft Propulsion Conference, ESA SP-465, 2000

[12]Laakso, H., Grard, R., Janhunen, P., Trotignon, J.-G., "Plasma and wave phenomena induced by neutral gas releases in the solar wind", Ann. Geophys., Vol. 20, No. 11, 2002, pp. 1–11

[13]Birdsall, C.K., and Langdon, A.B., "Plasma Physics via Computer Simulation", Institute of Physics Publishing, 1991

[14]Birdsall, C.K., "Particle-in-Cell Charged-Particle Simulations, Plus Monte Carlo Collisions With Neutral Atoms, PIC-MCC", *IEEE Transactions on Plasma Science*, **19**, No. 2, April 1991

[15]VanGilder, D. B., Boyd, I. D., Keidar, M., "Particle Simulations of a Hall Thruster Plume", *Journal of Spacecraft and Rockets*, Vol. 37, No. 1, Jan 2000

[16]Boyd, I. D., "Review of Hall Thruster Plume Modeling", Journal of Spacecraft and Rockets, Vol 38, No. 3, May-June 2001, and referenced therein: Dalgarno, A., MacDowell, M. R. C., Williams, A., "The Mobilities of Ions in Unlike Gases" Proceedings of the Royal Society, Vol 250, April 1958, pp. 411-425

[17]Rapp, D., Francis, W. E., "Charge Exchange between Gaseous Ions and Atoms", *The Journal of Chemical Physics*, Vol. 37, No. 11, Dec. 1962

[18]Miller, S. J., Pullins, S. H., Levandier, D. J., Chiu, Y., Dressler, R. A., "Xenon Charge Exchange Cross Sections for Electrostatic Thruster Models", *Journal of Applied Physics*, Vol. 91, No. 3, Feb. 2002

[19]Dressler, R. A., email conversation in May 2004

[20]King, L.B., Gallimore, A.D., "Identifying Charge-Exchange Collision Products within the Ion-Energy Distribution of Electrostatically Accelerated Plasmas", *Physics of Plasmas*, Vol. 6, No. 7, 1999, pp. 2936-2942

[21]King, L.B., Gallimore, A.D., "Mass Spectral Measurements in the Plume of an SPT-100 Hall Thruster", *Journal of Propulsion and Power*, Vol. 16, No. 6, 2000, pp. 1086-1092

[22]Tharamel, J., Kharchenko, V.A., and Delgarno, A., "Resonant Charge Transfer in Collisions between Positive Ions ", *Physical Review A*, Vol. 50, No. 1, 1994, pp. 496-501

[23]Materassi, M. (Project Leader), et al., "Final Report for Stentor Plasma Probe Extensive On Ground Characterization", Doc. No. TL 17106, Laben/Proel Tecnologie Division, Oct. 2000